Cell Reports
Report

Targeting Synthetic Lethal Interactions between Myc and the eIF4F Complex Impedes Tumorigenesis

Chen-Ju Lin,[1,9] Zeina Nasr,[1,9] Prem K. Premsrirut,[4] John A. Porco, Jr.,[5] Yoshitaka Hippo,[6] Scott W. Lowe,[2,7,8] and Jerry Pelletier[1,2,3,*]
[1]Department of Biochemistry
[2]Department of Oncology
[3]The Rosalind and Morris Goodman Cancer Research Center
McGill University, Montreal, Quebec H3G 1Y6, Canada
[4]Cold Spring Harbor Laboratories, Cold Spring Harbor, New York, NY 11724, USA
[5]Department of Chemistry, Center for Chemical Methodology and Library Development (CMLD-BU), Boston University, 590 Commonwealth Avenue, Boston, MA 02215, USA
[6]Division of Cancer Development System, National Cancer Center Research Institute, Tokyo 104-0045, Japan
[7]Howard Hughes Medical Institute, 4000 Jones Bridge Road, Chevy Chase, MD 20815-6789, USA
[8]Memorial Sloan-Kettering Cancer Center, 1275 York Avenue, New York, NY 10065, USA
[9]These authors contributed equally to this work
*Correspondence: jerry.pelletier@mcgill.ca
DOI 10.1016/j.celrep.2012.02.010

SUMMARY

The energetically demanding process of translation is linked to multiple signaling events through mTOR-mediated regulation of eukaryotic initiation factor (eIF)4F complex assembly. Disrupting mTOR constraints on eIF4F activity can be oncogenic and alter chemotherapy response, making eIF4F an attractive antineoplastic target. Here, we combine a newly developed inducible RNAi platform and pharmacological targeting of eIF4F activity to define a critical role for endogenous eIF4F in Myc-dependent tumor initiation. We find elevated Myc levels are associated with deregulated eIF4F activity in the prelymphomatous stage of the *Eμ-Myc* lymphoma model. Inhibition of eIF4F is synthetic lethal with elevated Myc in premalignant pre-B/B cells resulting in reduced numbers of cycling pre-B/B cells and delayed tumor onset. At the organismal level, eIF4F suppression affected a subset of normal regenerating cells, but this was well tolerated and rapidly and completely reversible. Therefore, eIF4F is a key Myc client that represents a tumor-specific vulnerability.

INTRODUCTION

The heterotrimeric eukaryotic initiation factor (eIF)4F complex catalyzes the rate-limiting step of translation initiation by stimulating ribosome recruitment to mRNA templates. This is achieved through the coordinated action of the eIF4E subunit (required for binding to mRNA 5′ cap [$^{5'}m^7GpppN^{3'}$] structures), ATP hydrolysis (mediated by two eIF4A isoforms [eIF4AI and eIF4AII]), and interaction between the eIF4G subunit and the 43S preinitiation complex. Different mRNAs show varying dependencies on eIF4F for ribosome recruitment—a feature attributed to accessibility of the mRNA 5′ cap (Dever, 2002). Altered signaling flux through the PI3K/Akt/mTOR pathway in human cancers is associated with changes in eIF4F levels and modification of the cancer cell proteome due to selective translational effects (Rajasekhar et al., 2003). When elevated, eIF4E, the rate-limiting subunit of eIF4F (Duncan et al., 1987), antagonizes Myc-induced apoptosis and cooperates with Myc in tumorigenesis (Li et al., 2003; Ruggero et al., 2004; Wendel et al., 2004). As well, Myc exerts profound effects on protein synthesis through regulation of ribosome biogenesis (van Riggelen et al., 2010) and transcriptional control of the three eIF4F subunits (Jones et al., 1996; Lin et al., 2008). Increases in eIF4F activity have been shown to selectively stimulate the expression of malignancy-related mRNAs by augmenting nucleo/cytoplasmic transport of Cyclin D1 (Rousseau et al., 1996) and translation of Mcl-1 (Wendel et al., 2007) and Myc (Lin et al., 2008). The recent description of a Myc/eIF4F transcription/translation-coupled mitogenic loop (Lin et al., 2008) prompted us to develop a trackable mouse model to assess the in vivo contribution of eIF4F to Myc-dependent tumor initiation.

RESULTS

Transient Suppression of eIF4E Delays Myc-Dependent Tumor Initiation

Mouse models provide valuable platforms for identifying and characterizing lesions that promote tumorigenesis and for testing the significance of effector pathways downstream of known oncogenes and/or tumor suppressors for their contribution to cancer development and/or maintenance (Schmitt

Cell PRESS
Open ACCESS

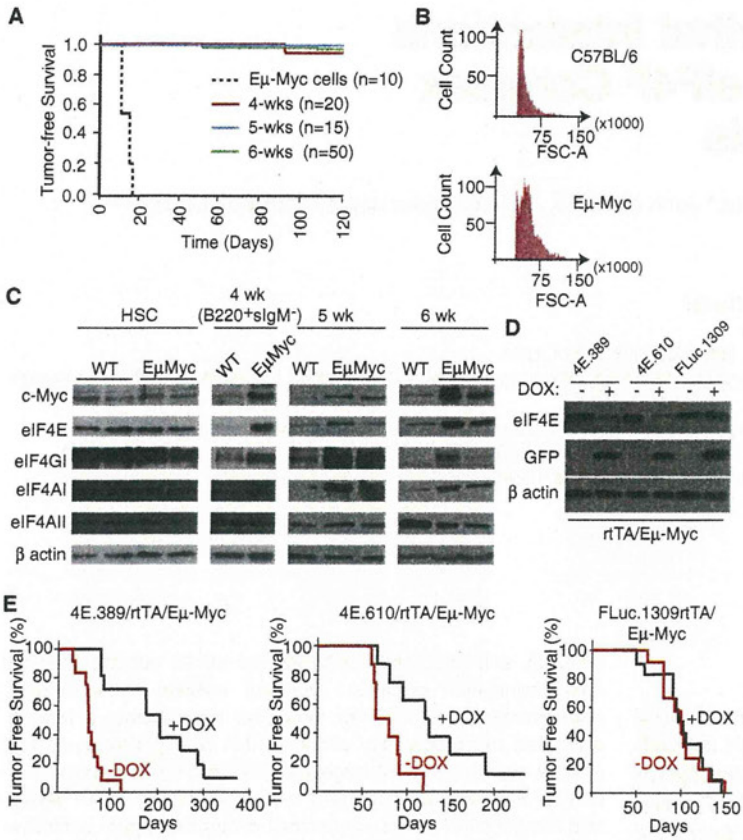

Figure 1. Transient Suppression of eIF4E Delays Myc-Dependent Tumor Initiation

(A) Kaplan-Meier plot illustrating tumor-free survival of recipient C57BL/6 mice transplanted with 20 *Eμ-Myc* lymphoma cells or 2 × 10^6 bone marrow cells from 4-, 5-, and 6-week-old *Eμ-Myc* mice.

(B) Forward light scatter from a flow cytometer of B220$^+$ splenocytes from 6-week-old C57BL/6 and *Eμ-Myc* mice. This assay was used as an independent validation to confirm the prelymphomatous nature of *Eμ-Myc* cells used in the transplantation experiments in (A).

(C) Western blot analysis of c-Myc transcriptional targets (eIF4E, eIF4AI, eIF4GI) in C57BL/6 (WT) and *Eμ-Myc* HSCs, B220$^+$sIgM$^-$ pre-B cells, and splenocytes from mice of the indicated ages.

(D) Suppression of eIF4E expression in B220$^+$ cells isolated from 6-week-old mice of the indicated genotype pretreated with vehicle or DOX for 2 weeks.

(E) Kaplan-Meier plot showing lymphoma-free survival of *4E.389/rtTA/Eμ-Myc* (n = 12), *4E.610/rtTA/Eμ-Myc* (n = 10), and *FLuc.1309/rtTA/Eμ-Myc* (n = 14) mice that had been treated with vehicle (red) or with DOX (black) for 21 days starting at 4 weeks of age.

See also Figure S1.

and Lowe, 2002). In the *Eμ-Myc* lymphoma model, Myc expression is driven by the lymphoid-specific IgH enhancer (Eμ) and becomes elevated in the pre-B/B cell compartment (Adams et al., 1985). Significant insight into Myc biology has been obtained using this model—from the finding that tumor-derived Myc mutants uncouple proliferation from apoptosis (Hemann et al., 2005) to the identification/characterization of ornithine decarboxylase, the rate-limiting enzyme for polyamine biosynthesis, as a Myc effector (Nilsson et al., 2005).

Sensitive transplantation assays of ostensibly healthy *Eμ-Myc* mice have shown that the majority (~90%) of *Eμ-Myc* donors, between 4 and 6 weeks of age, do not harbor malignant lymphoma cells (Langdon et al., 1986) (Figure 1A). In this prelymphomatous stage there is a polyclonal expansion of morphologically distinct pre-B cells (Figure 1B) that is offset by an increased apoptotic index (Jacobsen et al., 1994; Langdon et al., 1986). Subsequent acquisition of genetic lesions that block the cell death program triggers tumorigenesis (Strasser et al., 1990). Indeed, we have previously shown that enforced expression of eIF4E can drive aggressive cancers by attenuating apoptosis in this setting (Wendel et al., 2004). The *Eμ-Myc* mouse is thus a powerful model to study the contribution of Myc network components to tumor initiation, leading us to ask if perturbed eIF4F activity is a premalignant feature of *Eμ-Myc* pre-B/B cells.

To this end, we analyzed extracts from wild-type (WT) and *Eμ-Myc* hematopoietic stem cells (HSCs), 4 week B220$^+$sIgM$^-$, and 5–6 week splenic cells (Figure 1C). Myc expression is not elevated in *Eμ-Myc* HSCs but is appreciably increased in *Eμ-Myc* B220$^+$sIgM$^-$ B cells and splenocytes isolated from 4- to 6-week-old mice compared to WT controls (Figure 1C). The expression of all three eIF4F subunits is also increased in *Eμ-Myc* B220$^+$sIgM$^-$ B cells and splenocytes from 4- to 6-week-old mice relative to WT controls (Figure 1C). These results are consistent with previous studies indicating that eIF4E, eIF4AI, and eIF4GI, but not eIF4AII, are transcriptional targets of Myc (Jones et al., 1996; Lin et al., 2008) and demonstrate that eIF4F upregulation is a signature of premalignant *Eμ-Myc* preB/B lymphocytes.

To address whether elevated levels of eIF4F in *Eμ-Myc* pre-B/B cells represent an epigenetic change essential for tumor initiation, we took advantage of a powerful platform that combines optimized GFP-coupled small hairpin RNA (shRNA) technology with a Flp/FRT recombinase-mediated cassette exchange (RMCE) strategy to generate mice that conditionally express potent shRNAs targeting eIF4E (McJunkin et al., 2011; Premsrirut et al., 2011). Two independent miR-based shRNAs (shRNAmir) that target the eIF4E coding region, 4E.389 and 4E.610, and one that expresses a neutral control shRNAmir targeting Firefly Luciferase, FLuc.1309 (Premsrirut et al., 2011), were introduced into the FRT-hygro-pA "homing cassette" at the *Col1A1* locus of KH2 ES cells (see Figure S1A). These cells also harbor a reverse tet-transactivator (rtTA2) targeted to the *Rosa26* locus (referred to herein as *rtTA*) enabling potent, doxycycline (DOX)-inducible suppression of eIF4E (Figure S1B). Mice generated from these ES cells show inducible suppression of eIF4E in a wide spectrum of cells and tissues, including,

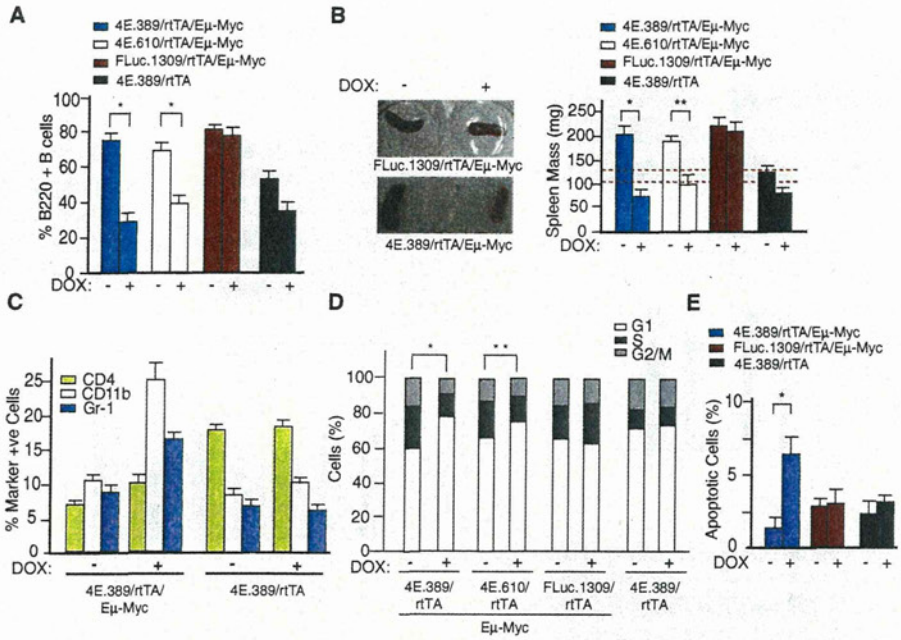

Figure 2. Inducible Suppression of eIF4E Reduces the B220⁺ B Cell Compartment, Impairs Cell Division, and Augments Apoptosis in Premalignant B Cells

(A) Flow cytometry analysis of B220⁺ B cells isolated from 6-week-old transgenic mice that had been treated with vehicle or DOX for 2 weeks. Error bars denote SEM (n = 3). *p < 0.002, as determined by the Student's t test.

(B) Representative photographs of spleens and average spleen mass of indicated 6-week-old triple-transgenic mice that had been treated with vehicle or DOX for 2 weeks. Red dotted lines represent the range of spleen masses from four 6-week-old control C57BL/6 mice. Error bars denote SEM (n = 4). *p < 0.001, **p < 0.01.

(C) Flow cytometry analysis of spleen cells isolated from *4E.389/rtTA/Eμ-Myc* mice and stained for the indicated cell surface markers. Each marker positive population was also >90% GFP+. Error bars are SEM (n = 3).

(D) Cell-cycle distribution of B220⁺ splenic B cells of the indicated genotype and DOX-treatment cohorts. Results are expressed as the average of three independent experiments (n = 3). *p < 0.01; **p < 0.05 for percent (%) G1 and S phase cells.

(E) In situ TUNEL analysis on freshly isolated splenic cells from 5 week transgenic mice that had been treated with vehicle or DOX for 6 days. Error bars denote SEM (n = 3). *p < 0.05.

See also Figure S2.

liver, spleen, skin, intestine, components of the hematopoietic system, and embryo-derived fibroblasts (Premsrirut et al., 2011) (Figures S1C and S1D; see below).

We crossed shRNAmir/rtTA and *Eμ-Myc* mice to generate triple-transgenic progeny in which eIF4E expression was suppressed during the prelymphomatous stage between 4 and 7 weeks of age. Robust induction of GFP expression and potent suppression of eIF4E was apparent in pre-B/B B220⁺ cells from *4E.389/rtTA/Eμ-Myc* and *4E.610/rtTA/Eμ-Myc* mice on DOX (Figure 1D). DOX-treated *4E.389/rtTA/Eμ-Myc* and *4E.610/rtTA/Eμ-Myc* mice showed a significant delay in lymphoma onset compared to either untreated controls or to DOX-treated *FLuc.1309/rtTA/Eμ-Myc* mice (Figure 1E; $p < 0.001$ for *4E.389/rtTA/Eμ-Myc* mice and $p < 0.01$ for *4E.610/rtTA/Eμ-Myc*). We attempted to assess the consequences of eIF4E suppression on tumor cell maintenance by administering DOX to 4-month-old lymphoma-bearing *4E.389/rtTA/Eμ-Myc* mice, but no stable response to disease was noted, and GFP induction was detected in only a minority of tumor cells (~8%–20%) (data not shown). This either reflects a collapse of the rtTA-inducible system as noted in other settings (Podsypanina et al., 2008), alterations in the DOX- or shelF4E-responsiveness of the target cell population, and/or weak or mosaic shelF4E expression—the latter having been documented in this shRNAmir/rtTA transgenic system (McJunkin et al., 2011). Nevertheless, our results indicate that endogenous eIF4E is required for conversion of *Eμ-Myc* pre-B/B cells to malignant lymphomas.

Suppression of eIF4E Reduces the B220⁺ *Eμ-Myc* Pre-B/B Cell Compartment by Impairing Cell Division and Apoptosis

To elucidate the mechanism(s) responsible for the delayed tumor onset, we analyzed the consequences of eIF4E suppression on the B cell population in the different transgenic settings (Figure 2). We observed a reduction in splenic (Figure 2A) and bone marrow-derived (Figure S2A) B220⁺ cells (1.8- to 2.5-fold) in DOX-treated *4E.389/rtTA/Eμ-Myc* and *4E.610/rtTA/Eμ-Myc* mice relative to vehicle-treated controls. As well, no significant

Cell PRESS
Open ACCESS

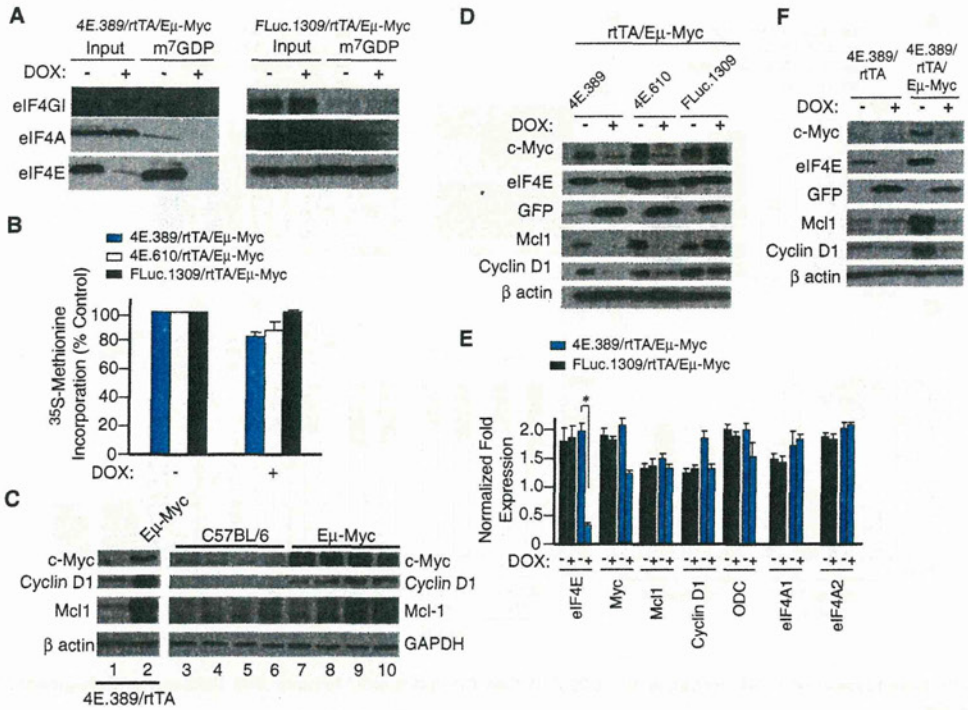

Figure 3. Inducible Suppression of eIF4E Impairs eIF4F Levels, Selectively Blocks Protein Synthesis, and Affects Production of Cyclin D1, Mcl-1, and Myc

(A) Relative abundance of the eIF4F complex in B220$^+$ cells from mice of the indicated genotype.

(B) Protein synthesis rates in B220$^+$ cells assessed by [^{35}S]methionine incorporation and TCA precipitation. Error bars denote SEM (n = 3).

(C) Western blot analysis of eIF4E-responsive targets in B220$^+$ cells isolated from 6-week-old mice. Cells were isolated from *4E.389/rtTA* (lane 1), *4E.389/rtTA/Eμ-Myc* (lane 2), and four independent C57BL/6 (lanes 3–6) or *Eμ-Myc* (lanes 7–10) mice.

(D) Western blot analysis showing reductions in Mcl-1, Cyclin D1, and Myc levels upon suppression of eIF4E in B220$^+$ cells in vivo.

(E) qRT-PCR quantitation of the indicated mRNA levels from B220$^+$ splenocytes (n = 6; *p = 0.003).

(F) Western blot analysis indicating levels of eIF4E targets upon eIF4E suppression in B220$^+$ cells.

See also Figure S3.

change in the pre-B/B cell population was observed in DOX-treated *FLuc.1309/rtTA/Eμ-Myc* mice, and a modest effect (<1.4-fold) was observed in DOX-treated *4E.389/rtTA* mice (Figures 2A and S2A). A significant reduction in spleen mass (>2-fold; *p < 0.001; **p < 0.01) in DOX-treated *4E.389/rtTA/Eμ-Myc* and *4E.610/rtTA/Eμ-Myc* mice was noted compared to vehicle-treated controls, DOX-treated *FLuc.1309/rtTA/Eμ-Myc* mice, or *4E.389/rtTA* mice (Figure 2B). The CD4$^+$ (T cells), CD11b$^+$ (monocyte/macrophages, granulocytes), and Gr-1$^+$ (granulocytes) cell populations were not depleted upon eIF4E suppression and even increased in some cases (Figure 2C). These results indicate that *Eμ-Myc* pre-B/B cells are exquisitely sensitive to eIF4E attenuation.

The differential effects of eIF4E inhibition on WT versus Myc overexpressing B cells appeared to be a consequence of impaired cell-cycle progression and increased apoptosis. The cell-cycle distribution of B220$^+$ cells was similar among all untreated triple-transgenic mouse strains but altered in B220$^+$ cells derived from DOX-treated *4E.389/rtTA/Eμ-Myc* and *4E.610/rtTA/Eμ-Myc* mice, both of which showed an accumulation in G1 phase and reductions in S/G2 phase populations (Figure 2D). Moreover, the percentage of apoptotic B220$^+$ cells in *4E.389/rtTA/Eμ-Myc* mice was increased upon DOX treatment compared to cells from vehicle-treated controls, DOX-treated *FLuc.1309/rtTA/Eμ-Myc*, or *4E.389/rtTA* mice (Figure 2E). Similar results were obtained in other settings—notably in murine 3T3 fibroblasts and human hTert-BJ cells, where coexpression of Myc and sheIF4E was associated with a proliferative disadvantage (Figures S2B and S2C) and increased apoptosis (Figure S2D). Taken together, these results indicate that eIF4E suppression and Myc overexpression share a synthetic lethal relationship that affects cell-cycle progression and survival.

Suppression of eIF4E Impairs eIF4F Complex Formation and Activity

Alterations in eIF4E levels lead to selective effects on translational output mediated through the eIF4F complex (Dever, 2002). To determine if eIF4F levels are perturbed in DOX-treated *4E.389/rtTA/Eμ-Myc* mice, B220$^+$ cells were isolated, and the eIF4F complex was purified by m^{7}GDP affinity chromatography (Figure 3A). Reductions in all three eIF4F subunits were noted in

DOX-treated *4E.389/rtTA/Eμ-Myc* B220$^+$ cells compared to cells from untreated *4E.389/rtTA/Eμ-Myc* or DOX-treated control *FLuc.1309/rtTA/Eμ-Myc* mice (Figure 3A). Metabolic labeling revealed only a modest reduction of ~20% in global protein synthesis in B220$^+$ cells from DOX-treated *4E.389/rtTA/Eμ-Myc* and *4E.610/rtTA/Eμ-Myc* mice (Figure 3B), with no alteration in the global profile of newly synthesized proteins (Figure S3A). Such results are consistent with what has been previously documented upon antisense suppression of eIF4E expression (Graff et al., 2007) and imply that the consequences on translation of altering eIF4E levels are due to its impact on specific mRNAs.

The effects of eIF4E suppression on pre-B/B cell-cycle progression and apoptosis (Figure 2) are consistent with previous observations that Cyclin D1, Myc, and Mcl-1 are particularly sensitive to eIF4E levels (Lin et al., 2008; Rosenwald et al., 1993; Wendel et al., 2007). Indeed, premalignant *Eμ-Myc* pre-B/B cells showed elevated levels of all three proteins (Figure 3C). Suppressing eIF4E expression led to reductions in the levels of all three eIF4E-responsive targets in splenic (Figure 3D) or bone marrow (Figure S3B) derived B220$^+$ cells isolated from DOX-treated *4E.389/rtTA/Eμ-Myc* and *4E.610/rtTA/Eμ-Myc*, but not from vehicle- or DOX-treated *FLuc.1309/rtTA/Eμ-Myc* mice. Reductions in Myc, Mcl-1, and Cyclin D1 protein levels observed upon eIF4E suppression are not a consequence of decreased transcript levels (Figure 3E) and were fully reversible upon removal of DOX (Figure S3C). In addition, eIF4E suppression had no consequences on expression from the eIF4E-insensitive β-actin, IRES-driven GFP (Balvay et al., 2007), and p27^{Kip1} mRNAs (Miskimins et al., 2001) (Figures 3D and S3D). Reductions in Mcl-1, Cyclin D1, and Myc upon eIF4E suppression were Myc context dependent in vivo because they were not observed in DOX-treated *4E.389/rtTA* cells (Figure 3F). These findings define eIF4E as a Myc client responsible for augmenting prosurvival and proliferative capacity through effectors, such as Mcl-1 and Cyclin D1.

Pharmacological Suppression of eIF4F Activity Blocks *Eμ-Myc*-Driven Tumor Initiation

To confirm and extend these genetic observations using a chemical biology approach, we took advantage of silvestrol, a small molecular inhibitor of the helicase activity of eIF4A, another essential component of the 4F complex (Bordeleau et al., 2008). Treatment of prelymphomatous *Eμ-Myc* mice for 3 weeks with silvestrol significantly delayed tumor onset (Figure 4A; $p < 0.01$). As noted for shRNA-mediated inhibition of eIF4E, silvestrol inhibited proliferation of *Eμ-Myc* pre-B/B cells, but not *Eμ-Myc* CD4$^+$ or CD11b$^+$ cells (Figures 4B and 4C). This was associated with a prolongation of G1 and shortening of S/G2 cell-cycle phases (Figure 4D), increased apoptosis (Figure 4E), and reductions in Mcl-1 and Cyclin D1 protein levels (Figure 4F). Whether the growth inhibitory effects of silvestrol were Myc context dependent was investigated utilizing NIH/3T3 cells ectopically expressing Myc/ER, a chimeric protein in which a mutant estrogen receptor (ER) ligand binding domain is fused to the carboxy-terminal domain of c-Myc. In this system, Myc/ER is constitutively expressed but only becomes active when 4-hydroxytamoxifen (4-OHT) is supplied (Littlewood et al., 1995). Indeed, NIH/3T3 cells were found to be more sensitive to silvestrol upon induction of Myc/ER by 4-OHT (Figure 4G). The convergence of genetic and pharmacological phenotypes confirms that Myc-expressing cells are sensitive to eIF4F inhibition.

Although the R26-rtTA allele is not ubiquitously expressed in the adult, it is well expressed in the gut and hematopoietic compartments, allowing us to assess toxicity in settings often most prone to drug-induced toxicities (Beard et al., 2006; Premsrirut et al., 2011). We noticed that when 4-week-old *4E.389/rtTA/Eμ-Myc* mice were treated with DOX for 2 weeks, a reduction in body weight was apparent within ~10 days (Figure S4A). Analysis of tissues with low proliferative indices that express GFP and sh4E.389 (i.e., liver; Figure S1C) showed no discernable histological changes (data not shown). In contrast a significant increase in apoptotic bodies in crypt epithelium, loss of goblet cells, and the presence of immature/undifferentiated crypts was apparent in intestines of DOX-treated *4E.389/rtTA/Eμ-Myc* mice (Figures S4B and S4C)—a tissue that displays strong GFP induction and efficient shRNA-mediated attenuation of expression by R26-rtTA (Figures S1C and S4B) (McJunkin et al., 2011; Premsrirut et al., 2011). These phenotypic changes were completely reversed upon DOX withdrawal (Figure S4B). No differences in Ki-67 staining in intestines from DOX- or vehicle-treated *4E.389/rtTA/Eμ-Myc* mice nor discernible histological changes in intestines from DOX- or vehicle-treated *FLuc.1309/rtTA/Eμ-Myc* mice were noticed (data not shown). Thus, although suppression of eIF4E has profound effects on some proliferating somatic tissues such as the intestine, these are well tolerated on the short term and are completely reversible without any discernible long-term negative impact on the animal's well-being.

DISCUSSION

Myc amplifications are frequent somatic copy-number alterations in human cancers (Beroukhim et al., 2010). The effectiveness of suppressing Myc as an anticancer therapeutic approach at the organismal level has been shown using dominant-negative forms of Myc (Soucek et al., 2008). Here, using both genetic and pharmacologic approaches, we demonstrate that the eIF4F complex functions as an essential Myc client during the initial phases of tumorigenesis. This relationship is likely in place for supporting normal B cell development where Mcl-1 has been shown essential for development of pro-B cells and later on, for maintenance of mature B lymphocytes (Opferman et al., 2003), in contrast to Bcl2, which appears largely dispensable for early pro-B, pre-B, and immature cell development (Kelly et al., 2007). The pre-B cell origin of sporadic *Eμ-Myc* lymphomas (Adams et al., 1985) is consistent with eIF4F being a Myc client—leading to upregulation of Mcl-1 expression.

We find that inhibition of eIF4F significantly delayed Myc-induced lymphomagenesis without overt toxicity to normal hematopoietic cells and other tissues. The transgenic model that we established did not allow us to probe the Myc-eIF4F relationship in tumor maintenance due to apparent collapse of the rtTA-inducible system (see above); however, we expect such a relationship to also be relevant in established tumors because curtailing eIF4F helicase activity with small molecule

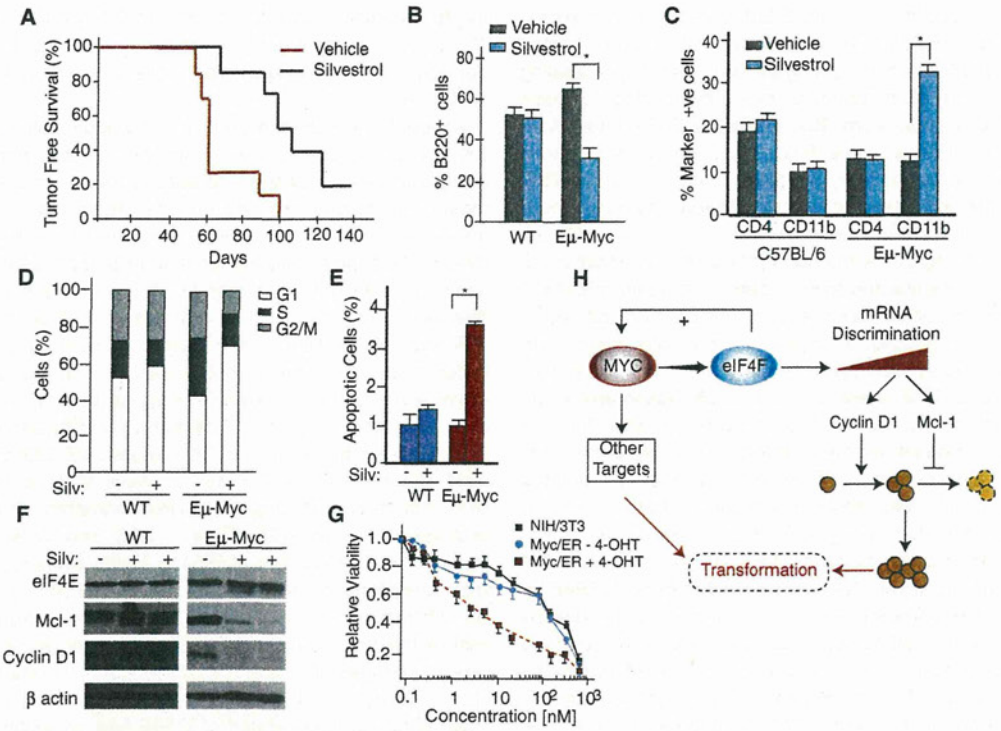

Figure 4. Blocking *Eμ-Myc*-Driven Tumor Initiation by Pharmacological Suppression of eIF4F Activity

(A) Kaplan-Meier plot showing lymphoma-free survival of 4-week-old *Eμ-Myc* mice treated with or without 0.2 mg/kg silvestrol ($n = 7$; $p < 0.01$) for 23 days.

(B) Percent $B220^+$ cells isolated from 6-week-old C57BL/6 or *Eμ-Myc* mice that had been treated with vehicle or silvestrol for 2 weeks. Error bar represent SEM ($n = 3$). $^*p < 0.01$.

(C) Percent $CD4^+$ and $CD11b^+$ cells isolated from 6-week-old C57BL/6 or *Eμ-Myc* mice that had been treated with vehicle or silvestrol for 2 weeks. Error bar represent SEM ($n = 3$). $^*p < 0.001$.

(D) Cell-cycle distribution of $B220^+$ splenic B cells of the indicated genotype and drug treatments. Results are expressed as the average of three independent experiments.

(E) In situ TUNEL analysis on freshly isolated splenic cells from 5-week-old mice that had been treated with vehicle or silvestrol for 6 days ($n = 3$ mice). $^*p < 0.001$.

(F) Western blot analysis of eIF4F targets in splenic $B220^+$ cells isolated from untreated or silvestrol-treated *Eμ-Myc* or C57BL/6 mice.

(G) Sensitivity of NIH/3T3 cells to silvestrol. NIH/3T3 or Myc/ER NIH 3T3 cells were exposed to vehicle or 250 nM 4-OHT for 18 hr and then to silvestrol for an additional 24 hr at the indicated concentrations. Cell viability was determined using the Sulforhodamine B (SRB) colorimetric assay and is set relative to vehicle-treated cells. Values represent the average of three biological replicates, and error bars denote SEM.

(H) Relationship among Myc, eIF4F, and eIF4E effectors leading to increased cell-cycle progression and survival advantage during the premalignant phase of lymphomagenesis. The plus (+) sign indicates that increased eIF4F levels also stimulate c-Myc mRNA translation (Lin et al., 2008).

See also Figure S4.

inhibitors (silvestrol or hippuristanol) (Cencic et al., 2009; Lucas et al., 2009; Tsumuraya et al., 2011) or suppression of eIF4E by systemic delivery of eIF4E antisense oligonucleotides (Graff et al., 2007) in xenograft models all show significant anticancer activity while not displaying overt cytotoxicity to nontransformed cells. As well, Myc lymphoma cells expressing shRNAs to eIF4E have a selective growth disadvantage (Mills et al., 2008), overexpression of eIF4E antagonizes Myc-dependent apoptosis (Li et al., 2003; Ruggero et al., 2004), and gene amplification along the Myc-eIF4F axis can evade mTOR- and PI3K-targeted therapy (Ilic et al., 2011; Wendel et al., 2004).

We have not observed a loss in body weight with the use of silvestrol even when administered daily for 4 weeks (data not shown), consistent with previous studies documenting that long-term administration of this compound is well tolerated—affecting neither spleen or liver weights, nor altering liver aminotransferase activity, and showing little effect on cells of the hematopoietic lineage (Cencic et al., 2009). This may pertain to differences in the degree/extent of translation inhibition achieved in vivo with single daily doses of silvestrol versus chronic suppression of eIF4E by DOX. Because silvestrol has a short serum half-life (~6 hr) (Saradhi et al., 2011), treatment with this compound would result in cycles consisting of a period of translation inhibition followed by recovery. This is in contrast to the chronic suppression of eIF4E expected from continuous administration of DOX to sheIF4E-expressing mice. Alternatively, differences in the downstream consequences on translation of inhibiting eIF4A versus eIF4E in vivo may also be contributing to the differences in toxicity. Hence, a key advantage of the shRNA system used herein is to predict on-target toxicities.

From the work presented here, we anticipate that eIF4F targeting drugs with increased potency may have increased intestinal toxicity, but such toxicities would be manageable.

Although previous studies have indicated that silvestrol can have anticancer effects (Bordeleau et al., 2008; Cencic et al., 2009; Lucas et al., 2009), the remarkable similarity between results produced through RNAi-mediated or chemical inhibition strongly suggests that silvestrol acts to limit cancer progression through targeting eIF4F. Of note, other recent efforts informed by RNAi or chemical biology-based screens have identified chromatin and SUMOylation modifiers required for Myc-driven tumorigenesis (Kessler et al., 2012; Mertz et al., 2011; Zuber et al., 2011). Consequently, whereas Myc has long been considered "undruggable," there are now several therapeutically viable options for selectively targeting Myc oncogenic functions in different contexts. Indeed, combination strategies using these approaches might achieve greater potency and potentially bypass resistance.

Regardless of these therapeutic possibilities, our studies demonstrate that Myc can exert a role in tumor maintenance via selective effects on the translation of specific mRNAs. The eIF4F complex preferentially stimulates the translation of a subset of mRNAs that harbors highly structured 5′ untranslated regions and that encodes regulators of cell growth, proliferation, and apoptosis (Koromilas et al., 1992; Larsson et al., 2007; Mamane et al., 2007). Large-scale changes to the cellular transcriptome, as executed upon Myc elevation, are expected to disproportionately alter the competitive ability of individual cellular mRNAs for limiting eIF4F levels, leading to distinctive translational changes (Dever, 2002). Our data indicate that Myc exploits eIF4F's mRNA discriminatory ability to selectively upregulate such effectors (Figure 4H). In this manner Myc coordinates changes in protein synthesis with its well-established nuclear activities, a feature that may be important for normal Myc function but that also creates an unnatural dependency under conditions of aberrant and/or sustained Myc levels.

EXPERIMENTAL PROCEDURES

Reagents, Cell Culture, and Mice

shRNAs targeting eIF4E were designed and tested as previously described (Paddison et al., 2004). Two of these, sh4E.389 (5′-TTAAATTACTAGACA ACTGGA-3′) and sh4E.610 (5′-TTTAGCTCTAACATTAACAAC-3′), as well as shFLuc.1309 (a neutral shRNA targeting Firefly luciferase; Premsrirut et al., 2011) were targeted to the murine Col1A1 locus using a Flp/FRT RMCE strategy in pre-engineered ES cells (Hochedlinger et al., 2005). All ES cells were selected and maintained on irradiated (40 Gy) MEFs derived from the DR4 mouse strain. ES cells were cultured in knockout Dulbecco's modified Eagle's medium (Cellgro Mediatech) supplemented with 10% fetal bovine serum (FBS), L-glutamine, penicillin-streptomycin, nonessential amino acid, LIF (leukemia inhibitory factor), and 55 μM β-mercaptoethanol. Electroporations with KH2 ES cells were performed with 50 μg pColTGM (aka CTGM) and 25 μg pCAGGS-FLPe at 400V and 125 μF as previously described (Premsrirut et al., 2011). ColAI-targeted clones were selected in hygromycin, tested for GFP inducibility, and transgenic mice derived using tetraploid embryo complementation.

Eμ-Myc mice were crossed to *4E.389/rtTA*, *4E.610/rtTA*, or *FLuc.1309/rtTA* mice to generate triple-transgenic mice. Genotypes were obtained at the expected Mendelian inheritance ratios. The *Eμ-Myc* transgene was detected by genomic PCR amplification of a 600 bp product using the primers 5′-GG ACAGTGCTTAGATCCAAGGTGA-3′ and 5′-CCTCTGTCTCTCGCTGGAATT ACT-3′. Genotyping for *R26-rtTA* was performed using the primers 5′-AA AGTCGCTCTGAGTTGTTAT-3′, 5′-GCGAAGAGTTTGTCCTCAACC-3′, and 5′-GGAGCGGGAGAAATGGATATG-3′. Genotyping for *R26-rtTA* yields two PCR products of ~500 bp (WT *ROSA26* allele) and ~300 bp (*R26-rtTA* allele). Genotyping for *4E.389* by PCR used the primers 5′-AATTACTAGACAACTG GATTGCCT-3′ and 5′-GAAGAACAATCAAGGGTCC-3′ (~200 bp product), whereas genotyping for *4E.610* by PCR used the primers 5′-GCCACAGA TGTATTTAGCTCTAAC-3′ and 5′-GAAGAACAATCAAGGGTCC-3′ (~200 bp product). Genotyping for *FLuc.1309* used the primers 5′-CACCCTGAAAA CTTTGCCCC-3′ and 5′-AAGCCACAGATGTATTAATCAGAGA-3′ (~300 bp product).

All mice strains were maintained on a C57BL/6 background. Activation of shRNAmir production in mice was performed in 4-week-old transgenic mice by supplying DOX (1 mg/ml) in the drinking water (plus 5% sucrose) for the indicated periods of time. DOX-supplemented water was changed every 4 days. To assess the impact of silvestrol on lymphoma onset, 4-week-old *Eμ-Myc* mice were treated with vehicle (5.2% PEG 400/5.2% Tween 80) or 0.2 mg/kg silvestrol (daily intraperitoneal injections) for 23 consecutive days. All mice were monitored twice a week for signs of morbidity and lymphoma development, the latter scored by peripheral lymph node palpation. Tumor-free survival is defined as the time from birth to the time of appearance of a palpable lymphoma. Data were analyzed in the Kaplan-Meier format using the log rank (Mantel-Cox) test for statistical significance. All animal studies were approved by the McGill University Faculty of Medicine Animal Care Committee.

Flow Cytometry

Fresh-cell suspensions were isolated in PBS plus 2% FBS. Erythrocytes were removed by lysis in ACK buffer (150 mM NH_4Cl, 10 mM $KHCO_3$, and 0.1 mM EDTA). Remaining cells were collected by centrifugation and resuspended in 1 ml PBS plus 2% FBS. Blocking was performed by incubating samples with purified anti-CD16/CD32 antibody (clone: 2.4G2; BD Biosciences) for 5 min on ice before labeling cells with fluorochrome-conjugated substrate-specific antibodies. The forward and side light-scatter gate excluded small apoptotic cells and granular cells, whereas large cells were included.

Antibodies used to identify monocytes and granulocytes were Ly-6G (Gr-1) PECy7 (clone 1A8; BD Biosciences) and CD11b PE (clone M1/70; BD Biosciences). Antibodies used to identify T and B lymphocytes were CD4 PE (clone RM4-5; BD Biosciences) and CD45R/B220 PE (clone RA3-6B2; BD Biosciences). Incubations were performed in the dark on ice for 20 min before data acquisition, and analyses were conducted on a FACSAria II (BD Biosciences). Erythrocytes, dead cells, and debris were excluded with gating based on forward/side-scatter characteristics. The percent B and T lymphocytes, monocytes, and granulocytes for each sample was expressed as a percentage of total gated cells analyzed.

To measure apoptosis in vivo, TUNEL assays were performed on freshly isolated splenic cells from indicated transgenic mice treated with vehicle or DOX for 6 days following the manufacturer's instructions (In Situ Cell Death Detection Kit, TMR red; Roche).

For cell-cycle analysis, freshly isolated splenic $B220^+$ cells from vehicle or DOX-treated transgenic mice were incubated with 1 ml DNA-staining buffer (0.3% Triton X-100, 50 μg/ml propidium iodine, 20 μg/ml RNase A, and 4 mM sodium citrate). Cell-cycle distribution was analyzed by flow cytometry using a Guava EasyCyte (Millipore).

For silvestrol-treated C57BL/6 and *Eμ-Myc* mice, freshly isolated splenic $B220^+$ cells (10^6 cells/ml) were washed, fixed in 75% ethanol solution for 1 hr at 4°C, and stained with propidium iodide (Sigma-Aldrich) (50 μg/ml propidium iodide, 3.8 mM sodium citrate, and 500 μg/ml RNase A) for 3 hr at 4°C. Cells were then analyzed for DNA content using a FACScan (BD Biosciences).

Expression Analysis

For western blotting, cells were lysed in RIPA lysis buffer (50 mM Tris-HCl [pH 7.5], 150 mM NaCl, 1 mM DTT, 0.1% SDS, 1% NP-40, 0.5% sodium deoxycholate, 0.1 mM phenylmethylsulfonyl fluoride [PMSF], 1 μg/ml each of leupeptin, pepstatin, and aprotinin). Protein concentrations were determined using the Bio-Rad Protein assay. Total protein lysates (30 μg) were

resolved by SDS-PAGE, transferred to PVDF membranes (Millipore), probed with the indicated antibodies, and visualized using enhanced chemiluminescence (ECL) detection (Amersham). Primary antibodies were as follows: anti-cyclin D1 was from Cell Signaling Technology (#2926; Beverly, MA, USA), and anti-Mcl-1 was purchased from AbD Serotec (#AHP1249; Oxford). Anti-GFP (#sc-9996), anti-eIF4E (#sc-9976), anti-p27 (#sc-528), and anti-c-Myc (#sc-764) antibodies were obtained from Santa Cruz Biotechnology. Anti-β-actin (#A5316) and anti-tubulin (#T5268) antibodies were purchased from Sigma-Aldrich.

For metabolic studies, 2×10^5 B220$^+$ cells were isolated from vehicle or DOX-treated triple-transgenic mice and seeded in 24-well plates. Cells from DOX-treated mice were maintained in 1 μg/ml DOX. Cells were cultured for 45 min in methionine-free medium, followed by 60 min in [^{35}S]methionine-containing medium (150–220 μCi/ml) supplemented with 10% dialyzed FCS, washed, and lysed in RIPA buffer. Proteins were TCA precipitated onto 3MM Whatman paper, and the amount of radioactivity was quantitated by scintillation counting. Values were normalized to total protein levels as determined by the Bradford assay.

For m^{7}GTP Sepharose pull-down assays, freshly isolated cells were harvested in 300 μl of Lysis Buffer (20 mM HEPES$_{7.5}$, 100 mM KCl, 1.0 mM EDTA, 1 mM DTT, 1 mM PMSF, and 0.2% Tween 20, 10 mM NaF and 20 mM β-glycerophosphate), and then subjected to three cycles of freeze-thaw. The lysate was then incubated with 50 μl of 50% slurry of m^{7}GTP-Sepharose 4B (GE Healthcare, UK) for 2 hr at 4°C. The resin was washed three times with 1 ml of Lysis Buffer and one time with buffer A containing 200 μM GDP. Finally, proteins bound to the resin were eluted with 80 μl of m^{7}GDP (1 mM) for 10 min on ice. Aliquots of the eluted fractions (25 μl) were resolved by SDS-PAGE (10% polyacrylamide) and analyzed by western blotting.

Immunohistochemistry and TUNEL Staining

Tissues were harvested, fixed in 10% formalin, and embedded in paraffin. Sections (5 μm) were then dewaxed and rehydrated through a graded series of alcohol washes to water. They were placed in 10 mM citric acid buffer (pH 6.0) and subjected to antigen retrieval by boiling for 15 min. Immunohistochemistry was performed using HRP/DAB Detection Kit (ab64261; Abcam) according to the manufacturer's instruction. Briefly, after incubation with blocking buffer for 1 hr and 3% hydrogen peroxide for 10 min, rabbit anti-eIF4E (catalog #9742; Cell Signaling) or rabbit anti-GFP (catalog #2555; Cell Signaling) was applied overnight at 4°C. Sections were washed with TBS-T (1 M Tris-HCl [pH 7.5], 1.5 M NaCl, and 1% Tween 20) and incubated with biotinylated goat anti-rabbit IgG for 30 min at room temperature. After washing with TBS-T, streptavidin peroxidase was added for 30 min at room temperature. The signals were developed using DAB chromogen as substrate at room temperature for 5 min. Sections were counterstained with hematoxylin, dehydrated, and mounted with Permount. Apoptosis was detected with the use of the "In situ Cell Death Detection Kit, POD" according to the manufacturer's recommendations (Roche). Tissue sections were analyzed using an Aperio ScanScope XT (Aperio Technologies, Vista, CA, USA).

SUPPLEMENTAL INFORMATION

Supplemental Information includes four figures and can be found with this article online at doi:10.1016/j.celrep.2012.02.010.

LICENSING INFORMATION

ACKNOWLEDGMENTS

We thank Patrick Sénéchal and Marilyn Carrier for excellent technical assistance. C-J.L. was supported by a McGill Faculty of Medicine Internal Studentship. This work was supported by the Canadian Institutes of Health Research (MOP-106530 to J.P.), the NIH (GM-073855 to J.A.P.), a NCI program project grant (CA087497-11 to S.W.L.), and the Mouse Models of Human Cancer Consortium (S.W.L). P.K.P. is a founder, chief executive officer, and shareholder of Mirimus Inc. S.W.L. is a founder of Mirimus Inc. and a member of its scientific advisory board.

Received: January 9, 2012
Revised: February 14, 2012
Accepted: February 23, 2012
Published online: March 29, 2012

REFERENCES

Adams, J.M., Harris, A.W., Pinkert, C.A., Corcoran, L.M., Alexander, W.S., Cory, S., Palmiter, R.D., and Brinster, R.L. (1985). The c-myc oncogene driven by immunoglobulin enhancers induces lymphoid malignancy in transgenic mice. Nature *318*, 533–538.

Balvay, L., Lopez Lastra, M., Sargueil, B., Darlix, J.L., and Ohlmann, T. (2007). Translational control of retroviruses. Nat. Rev. Microbiol. *5*, 128–140.

Beard, C., Hochedlinger, K., Plath, K., Wutz, A., and Jaenisch, R. (2006). Efficient method to generate single-copy transgenic mice by site-specific integration in embryonic stem cells. Genesis *44*, 23–28.

Beroukhim, R., Mermel, C.H., Porter, D., Wei, G., Raychaudhuri, S., Donovan, J., Barretina, J., Boehm, J.S., Dobson, J., Urashima, M., et al. (2010). The landscape of somatic copy-number alteration across human cancers. Nature *463*, 899–905.

Bordeleau, M.E., Robert, F., Gerard, B., Lindqvist, L., Chen, S.M., Wendel, H.G., Brem, B., Greger, H., Lowe, S.W., Porco, J.A., Jr., and Pelletier, J. (2008). Therapeutic suppression of translation initiation modulates chemosensitivity in a mouse lymphoma model. J. Clin. Invest. *118*, 2651–2660.

Cencic, R., Carrier, M., Galicia-Vázquez, G., Bordeleau, M.E., Sukarieh, R., Bourdeau, A., Brem, B., Teodoro, J.G., Greger, H., Tremblay, M.L., et al. (2009). Antitumor activity and mechanism of action of the cyclopenta[b]benzofuran, silvestrol. PLoS One *4*, e5223.

Dever, T.E. (2002). Gene-specific regulation by general translation factors. Cell *108*, 545–556.

Duncan, R., Milburn, S.C., and Hershey, J.W. (1987). Regulated phosphorylation and low abundance of HeLa cell initiation factor eIF-4F suggest a role in translational control. Heat shock effects on eIF-4F. J. Biol. Chem. *262*, 380–388.

Graff, J.R., Konicek, B.W., Vincent, T.M., Lynch, R.L., Monteith, D., Weir, S.N., Schwier, P., Capen, A., Goode, R.L., Dowless, M.S., et al. (2007). Therapeutic suppression of translation initiation factor eIF4E expression reduces tumor growth without toxicity. J. Clin. Invest. *117*, 2638–2648.

Hemann, M.T., Bric, A., Teruya-Feldstein, J., Herbst, A., Nilsson, J.A., Cordon-Cardo, C., Cleveland, J.L., Tansey, W.P., and Lowe, S.W. (2005). Evasion of the p53 tumour surveillance network by tumour-derived MYC mutants. Nature *436*, 807–811.

Hochedlinger, K., Yamada, Y., Beard, C., and Jaenisch, R. (2005). Ectopic expression of Oct-4 blocks progenitor-cell differentiation and causes dysplasia in epithelial tissues. Cell *121*, 465–477.

Ilic, N., Utermark, T., Widlund, H.R., and Roberts, T.M. (2011). PI3K-targeted therapy can be evaded by gene amplification along the MYC-eukaryotic translation initiation factor 4E (eIF4E) axis. Proc. Natl. Acad. Sci. USA *108*, E699–E708.

Jacobsen, K.A., Prasad, V.S., Sidman, C.L., and Osmond, D.G. (1994). Apoptosis and macrophage-mediated deletion of precursor B cells in the bone marrow of E mu-myc transgenic mice. Blood *84*, 2784–2794.

Jones, R.M., Branda, J., Johnston, K.A., Polymenis, M., Gadd, M., Rustgi, A., Callanan, L., and Schmidt, E.V. (1996). An essential E box in the promoter of the gene encoding the mRNA cap-binding protein (eukaryotic initiation factor 4E) is a target for activation by c-myc. Mol. Cell. Biol. *16*, 4754–4764.

Kelly, P.N., Puthalakath, H., Adams, J.M., and Strasser, A. (2007). Endogenous bcl-2 is not required for the development of Emu-myc-induced B-cell lymphoma. Blood *109*, 4907–4913.

Kessler, J.D., Kahle, K.T., Sun, T., Meerbrey, K.L., Schlabach, M.R., Schmitt, E.M., Skinner, S.O., Xu, Q., Li, M.Z., Hartman, Z.C., et al. (2012). A SUMOylation-dependent transcriptional subprogram is required for Myc-driven tumorigenesis. Science *335*, 348–353.

Koromilas, A.E., Lazaris-Karatzas, A., and Sonenberg, N. (1992). mRNAs containing extensive secondary structure in their 5′ non-coding region translate efficiently in cells overexpressing initiation factor eIF-4E. EMBO J. *11*, 4153–4158.

Langdon, W.Y., Harris, A.W., Cory, S., and Adams, J.M. (1986). The c-myc oncogene perturbs B lymphocyte development in E-mu-myc transgenic mice. Cell *47*, 11–18.

Larsson, O., Li, S., Issaenko, O.A., Avdulov, S., Peterson, M., Smith, K., Bitterman, P.B., and Polunovsky, V.A. (2007). Eukaryotic translation initiation factor 4E induced progression of primary human mammary epithelial cells along the cancer pathway is associated with targeted translational deregulation of oncogenic drivers and inhibitors. Cancer Res. *67*, 6814–6824.

Li, S., Takasu, T., Perlman, D.M., Peterson, M.S., Burrichter, D., Avdulov, S., Bitterman, P.B., and Polunovsky, V.A. (2003). Translation factor eIF4E rescues cells from Myc-dependent apoptosis by inhibiting cytochrome c release. J. Biol. Chem. *278*, 3015–3022.

Lin, C.J., Cencic, R., Mills, J.R., Robert, F., and Pelletier, J. (2008). c-Myc and eIF4F are components of a feedforward loop that links transcription and translation. Cancer Res. *68*, 5326–5334.

Littlewood, T.D., Hancock, D.C., Danielian, P.S., Parker, M.G., and Evan, G.I. (1995). A modified oestrogen receptor ligand-binding domain as an improved switch for the regulation of heterologous proteins. Nucleic Acids Res. *23*, 1686–1690.

Lucas, D.M., Edwards, R.B., Lozanski, G., West, D.A., Shin, J.D., Vargo, M.A., Davis, M.E., Rozewski, D.M., Johnson, A.J., Su, B.N., et al. (2009). The novel plant-derived agent silvestrol has B-cell selective activity in chronic lymphocytic leukemia and acute lymphoblastic leukemia in vitro and in vivo. Blood *113*, 4656–4666.

Mamane, Y., Petroulakis, E., Martineau, Y., Sato, T.A., Larsson, O., Rajasekhar, V.K., and Sonenberg, N. (2007). Epigenetic activation of a subset of mRNAs by eIF4E explains its effects on cell proliferation. PLoS One *2*, e242.

McJunkin, K., Mazurek, A., Premsrirut, P.K., Zuber, J., Dow, L.E., Simon, J., Stillman, B., and Lowe, S.W. (2011). Reversible suppression of an essential gene in adult mice using transgenic RNA interference. Proc. Natl. Acad. Sci. USA *108*, 7113–7118.

Mertz, J.A., Conery, A.R., Bryant, B.M., Sandy, P., Balasubramanian, S., Mele, D.A., Bergeron, L., and Sims, R.J., 3rd. (2011). Targeting MYC dependence in cancer by inhibiting BET bromodomains. Proc. Natl. Acad. Sci. USA *108*, 16669–16674.

Mills, J.R., Hippo, Y., Robert, F., Chen, S.M., Malina, A., Lin, C.J., Trojahn, U., Wendel, H.G., Charest, A., Bronson, R.T., et al. (2008). mTORC1 promotes survival through translational control of Mcl-1. Proc. Natl. Acad. Sci. USA *105*, 10853–10858.

Miskimins, W.K., Wang, G., Hawkinson, M., and Miskimins, R. (2001). Control of cyclin-dependent kinase inhibitor p27 expression by cap-independent translation. Mol. Cell. Biol. *21*, 4960–4967.

Nilsson, J.A., Keller, U.B., Baudino, T.A., Yang, C., Norton, S., Old, J.A., Nilsson, L.M., Neale, G., Kramer, D.L., Porter, C.W., and Cleveland, J.L. (2005). Targeting ornithine decarboxylase in Myc-induced lymphomagenesis prevents tumor formation. Cancer Cell *7*, 433–444.

Opferman, J.T., Letai, A., Beard, C., Sorcinelli, M.D., Ong, C.C., and Korsmeyer, S.J. (2003). Development and maintenance of B and T lymphocytes requires antiapoptotic MCL-1. Nature *426*, 671–676.

Paddison, P.J., Caudy, A.A., Sachidanandam, R., and Hannon, G.J. (2004). Short hairpin activated gene silencing in mammalian cells. Methods Mol. Biol. *265*, 85–100.

Podsypanina, K., Politi, K., Beverly, L.J., and Varmus, H.E. (2008). Oncogene cooperation in tumor maintenance and tumor recurrence in mouse mammary tumors induced by Myc and mutant Kras. Proc. Natl. Acad. Sci. USA *105*, 5242–5247.

Premsrirut, P.K., Dow, L.E., Kim, S.Y., Camiolo, M., Malone, C.D., Miething, C., Scuoppo, C., Zuber, J., Dickins, R.A., Kogan, S.C., et al. (2011). A rapid and scalable system for studying gene function in mice using conditional RNA interference. Cell *145*, 145–158.

Rajasekhar, V.K., Viale, A., Socci, N.D., Wiedmann, M., Hu, X., and Holland, E.C. (2003). Oncogenic Ras and Akt signaling contribute to glioblastoma formation by differential recruitment of existing mRNAs to polysomes. Mol. Cell *12*, 889–901.

Rosenwald, I.B., Lazaris-Karatzas, A., Sonenberg, N., and Schmidt, E.V. (1993). Elevated levels of cyclin D1 protein in response to increased expression of eukaryotic initiation factor 4E. Mol. Cell. Biol. *13*, 7358–7363.

Rousseau, D., Kaspar, R., Rosenwald, I., Gehrke, L., and Sonenberg, N. (1996). Translation initiation of ornithine decarboxylase and nucleocytoplasmic transport of cyclin D1 mRNA are increased in cells overexpressing eukaryotic initiation factor 4E. Proc. Natl. Acad. Sci. USA *93*, 1065–1070.

Ruggero, D., Montanaro, L., Ma, L., Xu, W., Londei, P., Cordon-Cardo, C., and Pandolfi, P.P. (2004). The translation factor eIF-4E promotes tumor formation and cooperates with c-Myc in lymphomagenesis. Nat. Med. *10*, 484–486.

Saradhi, U.V., Gupta, S.V., Chiu, M., Wang, J., Ling, Y., Liu, Z., Newman, D.J., Covey, J.M., Kinghorn, A.D., Marcucci, G., et al. (2011). Characterization of silvestrol pharmacokinetics in mice using liquid chromatography-tandem mass spectrometry. AAPS J. *13*, 347–356.

Schmitt, C.A., and Lowe, S.W. (2002). Apoptosis and chemoresistance in transgenic cancer models. J. Mol. Med. *80*, 137–146.

Soucek, L., Whitfield, J., Martins, C.P., Finch, A.J., Murphy, D.J., Sodir, N.M., Karnezis, A.N., Swigart, L.B., Nasi, S., and Evan, G.I. (2008). Modelling Myc inhibition as a cancer therapy. Nature *455*, 679–683.

Strasser, A., Harris, A.W., Bath, M.L., and Cory, S. (1990). Novel primitive lymphoid tumours induced in transgenic mice by cooperation between myc and bcl-2. Nature *348*, 331–333.

Tsumuraya, T., Ishikawa, C., Machijima, Y., Nakachi, S., Senba, M., Tanaka, J., and Mori, N. (2011). Effects of hippuristanol, an inhibitor of eIF4A, on adult T-cell leukemia. Biochem. Pharmacol. *81*, 713–722.

van Riggelen, J., Yetil, A., and Felsher, D.W. (2010). MYC as a regulator of ribosome biogenesis and protein synthesis. Nat. Rev. Cancer *10*, 301–309.

Wendel, H.G., De Stanchina, E., Fridman, J.S., Malina, A., Ray, S., Kogan, S., Cordon-Cardo, C., Pelletier, J., and Lowe, S.W. (2004). Survival signalling by Akt and eIF4E in oncogenesis and cancer therapy. Nature *428*, 332–337.

Wendel, H.G., Silva, R.L., Malina, A., Mills, J.R., Zhu, H., Ueda, T., Watanabe-Fukunaga, R., Fukunaga, R., Teruya-Feldstein, J., Pelletier, J., and Lowe, S.W. (2007). Dissecting eIF4E action in tumorigenesis. Genes Dev. *21*, 3232–3237.

Zuber, J., Shi, J., Wang, E., Rappaport, A.R., Herrmann, H., Sison, E.A., Magoon, D., Qi, J., Blatt, K., Wunderlich, M., et al. (2011). RNAi screen identifies Brd4 as a therapeutic target in acute myeloid leukaemia. Nature *478*, 524–528.

WJGE World Journal of Gastrointestinal Endoscopy

Online Submissions: http://www.wjgnet.com/esps/
wjge@wjgnet.com
doi:10.4253/wjge.v4.i12.561

World J Gastrointest Endosc 2012 December 16; 4(12): 561-564
ISSN 1948-5190 (online)

BRIEF ARTICLE

Relationship of human rectal aberrant crypt foci and formation of colorectal polyp: One-year following up after polypectomy

Hirokazu Takahashi, Eiji Yamada, Hidenori Ohkubo, Eiji Sakai, Takuma Higurashi, Takashi Uchiyama, Kunihiro Hosono, Hiroki Endo, Atsushi Nakajima

Hirokazu Takahashi, Eiji Yamada, Hidenori Ohkubo, Eiji Sakai, Takuma Higurashi, Takashi Uchiyama, Kunihiro Hosono, Hiroki Endo, Atsushi Nakajima, Gastroenterology Division, Yokohama City University Graduate School of Medicine, Yokohama 236-0004, Japan

Author contributions: Takahashi H designed the study and wrote the manuscript; Yamada E, Ohkubo H, Sakai E, Higurashi T and Uchiyama T performed the colonoscopy; Hosono K and Endo H provided the collection of physical and imaging findings; Nakajima A providing appropriate advice for this work.

Supported by Grant-in-Aid for Research on the Third Term Comprehensive Control Research for Cancer from the Ministry of Health, Labour and Welfare, Japan to Nakajima A; a grant from the National Institute of Biomedical Innovation (NBIO) to Nakajima A; a grant from the Ministry of Education, Culture, Sports, Science and Technology, Japan (KIBAN-B) to Nakajima A and (KIBAN-C) to Takahashi H

Correspondence to: Hirokazu Takahashi, MD, Gastroenterology Division, Yokohama City University Graduate School of Medicine, 3-9 Fuku-ura, Kanazawa-ku, Yokohama 236-0004, Japan. hirokazu@med.yokohama-cu.ac.jp
Telephone: +81-45-7872640 Fax: +81-45-7843546

Received: October 13, 2011 Revised: October 20, 2012
Accepted: December 1, 2012
Published online: December 16, 2012

Abstract

AIM: To clarify the relationship of human rectal aberrant crypt foci and formation of colorectal polyp.

METHODS: Eighty-nine subjects were recruited from the population of Japanese individuals who underwent polypectomy at Yokohama City University Hospital. All patients had baseline adenomas removed at year 0 colonoscopy. Aberrant crypt foci (ACF) were defined as lesions in which the crypts were more darkly stained with methylene blue than normal crypts and had larger diameters, often with oval or slit-like lumens and a thicker epithelial lining.

RESULTS: A total of 366 ACFs were identified in 89 patients; all had baseline adenomas removed at the first examination (year 0) colonoscopy and returned for the second (year 1). ACF in the lower rectum were assessed at year 0 and study group were divided into two groups depend on ACF numbers, 0-3 or over 3. All participants were examined in the number and maximum size of adenoma. There was no statistical difference in number and maximum size of ACF at year 0, however, maximum size of adenoma was larger in over 3 group than 0-3 group at year 1.

CONCLUSION: The number of ACF may be a predictive factor of relatively large adenoma incidence in the pilot phase study.

Key words: Aberrant crypt foci; Colorectal carcinogenesis; Visceral fat; Adiponectin

Peer reviewer: Shuhei Yoshida, MD, PhD, Division of Gastroenterology, Beth Israel Deaconess Medical Center, Harvard Medical School, 330 Brookline Ave, Boston, MA 02215, United State

Takahashi H, Yamada E, Ohkubo H, Sakai E, Higurashi T, Uchiyama T, Hosono K, Endo H, Nakajima A. Relationship of human rectal aberrant crypt foci and formation of colorectal polyp: One-year following up after polypectomy. *World J Gastrointest Endosc* 2012; 4(12): 561-564 Available from: URL: http://www.wjgnet.com/1948-5190/full/v4/i12/561.htm DOI: http://dx.doi.org/10.4253/wjge.v4.i12.561